Evaluation of Fluoro-Jade C staining: specificity and application to damaged immature neuronal cells in the normal and injured mouse brain

Takuya Ikenari[1], Hirofumi Kurata[1,2,3], Takemasa Satoh[4], Yoshio Hata[4,5], Tetsuji Mori[1]

[1] Department of Biological Regulation, School of Health Science, Faculty of Medicine, Tottori University, Yonago, 683-8503, Japan

[2] Division of Child Neurology, Department of Brain and Neurosciences, Faculty of Medicine, Tottori University, Yonago, 683-8504, Japan

[3] Department of Pediatrics, National Hospital Organization, Kumamoto Saishunso National Hospital, Koshi, 861-1196, Japan

[4] Division of Neurobiology, School of Life Sciences, Faculty of Medicine, Tottori University Yonago, 683-8503, Japan

[5] Division of Integrative Bioscience, Institute of Regenerative Medicine and Biofunction, Tottori University Graduate School of Medical Sciences, Yonago, 683-8503, Japan

Corresponding author

Tetsuji Mori

Department of Biological Regulation, School of Health Science, Faculty of Medicine, Tottori University, Yonago, 683-8503, Japan

Tel. and Fax: +81-859-38-6352, E-mail: mori-te@tottori-u.ac.jp

Abstract

Fluoro-Jade C (FJC) staining is widely used for the specific detection of all degenerating mature neurons, including apoptotic, necrotic, and autophagic cells. However, whether FJC staining can detect degenerating immature neurons and neural stem/precursor cells remains unclear. In addition, some conflicting studies have shown that FJC and its ancestral dyes, Fluoro-Jade (FJ) and FJB, can label resting/activated astrocytes and microglia. In the present study, we examined the validity of FJC staining for the detection of neuronal cells in adult and embryonic mouse brains under normal and injured conditions. In the adult rodent subventricular zone-rostral migratory stream-olfactory bulb system, apoptosis associated with neurogenesis occurs under normal conditions. Using this system, we detected FCJ positive (+) cells, some of which were doublecortin (DCX)(+) neuroblasts, in addition to neuronal nuclei (NeuN)(+) mature neurons. FJC negative (-) apoptotic cells expressing activated Caspase 3 were also observed, and a small number of FJC(+)/ionized calcium-binding adaptor 1 (Iba1)(+) microglia and FJC(+)/glial fibrillary acidic protein (GFAP)(+) astrocytes were observed in the normal brain. Next, we analyzed embryonic brains, in which the apoptosis of neural stem/precursor cells was induced by the administration of N-ethyl-N-nitrosourea (ENU) or ethanol at embryonic day 14 or 10, respectively. In those brains, FJC(+) neural stem/precursor cells and neuroepithelial cells expressing SRY-related HMG-box 2 (Sox2) were observed. Surprisingly degenerating mesenchymal cells were also FJC(+). The present study indicates that FJC is a reliable marker for degenerating neuronal cells during all differentiation stages. However, FJC could also label degenerating non-neuronal cells under some conditions.

Highlights

- Fluoro-Jade C can label degenerating immature neurons during adult neurogenesis under normal conditions.
- Fluoro-Jade C can label neural stem/precursor cells in apoptosis-induced embryonic brains.
- Some degenerating microglia and astrocytes can be Fluoro-Jade C positive under some conditions.
- Apoptotic mesenchymal cells induced by the administration of a toxic dose of ethanol were also Fluoro-Jade C positive.

Keywords

cell death, neural stem/precursor cells, adult neurogenesis, embryonic brain, glia, mesenchymal cells

Abbreviations

Cas3, activated Caspase3

DCX, doublecortin

ENU, N-ethyl-N-nitrosourea

FJ, Fluoro-Jade

GABA, gamma-aminobutyric acid

GAD67, glutamic acid decarboxylase 67

GFAP, glial fibrillary acidic protein

GFP, green fluorescent protein

Iba1, ionized calcium-binding adaptor molecule 1

ML, mantle layer

OB, olfactory bulb

PBS, phosphate buffered saline

PFA, paraformaldehyde

RMS, rostral migratory stream

Sox2, SRY-related HMG-box 2

SVZ, subventricular zone

TUNEL, TdT-mediated dUTP nick-end labeling

VZ, ventricular zone

(+), positive

(-), negative

Introduction

Neurons are vulnerable to many insults, including ischemia, traumatic injury, and excitotoxicity. Elucidating the mechanisms underlying neuronal cell death in the central nervous system is important because neurons are extremely difficult to regenerate, and the detection of degenerating neurons is necessary for many research fields. To detect degenerating neurons, suppressed silver techniques and hematoxylin and eosin staining have been used. However, these methods are not always able to accurately detect degenerating neurons due to the presence of artifacts and false positives (Cammermeyer, 1961; Ishida et al., 2004). In 1997, Fluoro-Jade (FJ) was reported as an alternative detection method for degenerating neurons (Schmued et al., 1997). In recent years, Fluoro-Jade B (FJB) and Fluoro-Jade C (FJC) have been developed, providing higher intensity and increased resolution for the identification of damaged neurons (Schmued and Hopkins, 2000; Schmued et al., 2005). FJs (FJ, FJB, and FJC) can visualize the cell bodies and processes of degenerating neurons in green florescence. The greatest advantage of FJs is that they can specifically detect degenerating neurons regardless of the manner of cell death, including necrosis, apoptosis, and autophagy (Krinke et al., 2001; Ballok et al., 2003; Shi et al., 2012). Moreover, FJs are more flexible and easier to use than conventional methods. In addition, FJs can be combined with immunostaining and can be applied not only to tissue sections but also to cultured cells (Gu et al., 2014). Currently, FJC is widely used to detect degenerating neurons (Shi et al., 2007; Wang et al., 2008; Knapp et al., 2014). Although FJs represent reliable staining techniques and it is believed that

FJs respond to molecular structures that are specific to degenerating neurons (Schmued et al., 1997), the detail mechanisms through which FJs identify degenerating neurons remain unclear.

Many studies have utilized FJC to detect degenerating mature neurons; however, studies using FJC in immature neurons remain limited. The subventricular zone (SVZ) of the adult rodent brain is an area where neurons are produced throughout life. Neural stem cells (Type-B cells) reside in the adult SVZ, and they sequentially differentiate into transient amplifying cells (Type-C cells) and neuroblasts (Type-A cells), which migrate through the rostral migratory stream (RMS) before differentiating into neurons in the olfactory bulb (OB) (Altman, 1969; Lois and Alvarez-Buylla, 1994; Doetsch et al., 1997). The SVZ-RMS-OB system is composed of many types of cells, including astrocytes, microglia, mature neurons, and endothelial cells (Jankovski and Sotelo, 1996; Ribeiro Xavier et al., 2015; Azevedo et al., 2017; Saito et al., 2018). During this process, approximately half of newly generated cells are eliminated through apoptosis (Biebl et al., 2000). Although FJB and FJC positive (+) cells have been observed in the SVZ-RMS-OB system (Mitrušková et al., 2005; Račeková et al., 2009), which cell types are being labeled by FJs remain unclear. In addition, although many studies have examined neuronal cell death in tissue sections from embryonic brains, few studies have utilized FJC. Gu et al. reported that *in vitro* neurotoxicity-induced degenerating neural stem cells were FJC(+) (Gu et al., 2014), but further *in vivo* analysis are necessary.

In addition, although FJs have been used to specifically stain degenerating neurons, some reports have indicated that FJ and/or FJB can detect reactive astrocytes and activated microglia (Colombo and Puissant,

2002; Damjanac et al., 2007), resting astrocytes in the spinal cord (Anderson et al., 2003), and non-degenerating neurons in the embryonic brain (Fernandes et al., 2004). Although FJC appears to be more specific to degenerating neurons than FJ and FJB, FJC has been reported to label resting and/or reactive astrocytes (Schmued et al., 2005; Brown and Sawchenko, 2007; Chidlow et al., 2009; Ehara and Ueda, 2009). Based on these reports, determining whether FJC staining is exclusive to degenerating neurons is necessary.

In this study, we examined whether FJC can detect the degeneration of immature neurons and neural stem/precursor cells in adult and embryonic brains. In addition, we determined the reactivity of FJC with astrocytes and microglia in normal and injured adult mouse brains.

Experimental procedures

Animals

Male and female ICR mice and GAD67-GFP transgenic mice (Tamamaki et al., 2003) older than six weeks old were used to analyze the adult brain. GAD67-GFP mice were maintained on a C57black/6 background. Timed pregnant ICR mice were used to analyze the embryonic brain. The day when a vaginal plug was detected was defined as gestational and embryonic day 0 (G0 and E0, respectively). Mice were supplied by Japan SLC (Hamamatsu, Japan). Mice were maintained under 12-h light/dark cycles. All experiments were performed in compliance with the Guidelines for Animal Experimentation of the Faculty of Medicine, Tottori University under the

International Guiding Principles for Biomedical Research Involving Animals. All experiments were approved by the Animal Care and Use Committee of Tottori University (approval number: 18-Y-45)

Animal treatments

ENU treatment

N-ethyl-N-nitrosourea (ENU, Sigma, St. Louis, MO, USA) was injected into pregnant mice on G13, as described previously (Leonard et al., 2001). Briefly, 1 g of ENU was dissolved in 10 mL of 95% ethanol and diluted with 90 ml of phosphate/citrate buffer (pH 5.0) and was administrated intraperitoneally (ip) to pregnant mice at a dose of 25 mg/kg. Embryos at E14 were fixed 24 h after the ENU injection, as described below. ENU was freshly prepared on the injection day. Untreated, age-matched control embryos were fixed at the same time.

Ethanol treatment

Ethanol was injected into pregnant mice on G9.5, as described previously (Dunty et al., 2001). Briefly, 25% ethanol in phosphate buffered saline (PBS), at a dose of 4.0 g/kg, was administered twice every 4 h. Embryos at E10 were fixed 12 h after the last administration, as described below. Untreated, age-matched control embryos were fixed at the same time.

Stab injury

Adult male mice were anesthetized by the ip injection of a mixture of medetomidine (0.3 mg/kg), midazolam (4 mg/kg) and butorphanol (5 mg/kg) in PBS. A small hole was made in the cranial bone, and the unilateral cerebral cortex was

scratched with tweezers. After surgery, the scalp was sutured, and mice survived for 24 h or 4 days. Injured mice were fixed, as described below.

Tissue preparation

Adult mice were euthanized by pentobarbital (200 mg/kg, ip) and perfused transcardially with PBS, followed by 4% paraformaldehyde in PBS (4% PFA/PBS). The brains and spinal cords were removed and postfixed with the same fixative overnight at 4°C. The spinal cords were embedded in 15% fish gelatin/PBS, and solidified with 4% PFA/PBS for 6 h at 4°C. Pregnant female mice were euthanized by cervical dislocation, and the embryonic heads were washed in PBS three times and fixed by immersion in 4% PFA/PBS for 6 hours at 4°C. Then, embryonic brains were removed. Fixed tissues were washed three times in three days with PBS to remove residual fixative, cryoprotected with 20% sucrose in PBS, embedded in Super Cryo Mount (Muto Pure Chemicals, Tokyo, Japan), snap frozen on dry ice, and cut using a cryostat.

Coronal sections, 12-µm-thick, were attached to gelatin-coated glass slides for the embryonic brain analysis, 30-µm-thick free-floating sections were used for the adult brain analysis, and 50-µm-thick free-floating sections were used for adult spinal cord analysis.

Primary antibody characterization

The primary antibodies used in this study are listed in Table 1.

The rabbit anti-activated Caspase-3 (Cas3) antibody (Promega, Madison, WI; Cat. # G748A, RRID:AB_430875) specifically recognizes apoptotic cells determined by TUNEL staining (Goodyear et al., 2014). In the present study,

Cas3 antibody stained only pyknotic nuclei determined by Hoechst33258 staining.

The guinea pig anti-DCX antibody (Millipore, Temecula, CA, USA; Cat. # AB2253, RRID:AB_10014654) recognize a single band at 45 kDa on western blotting of rat brain lysate (manufacturer's information). We obtained similar staining pattern as previous studies (Brandt et al., 2003; Takamori et al., 2014).

The specificity of the mouse anti-glial fibrillary acidic protein (GFAP) antibody (Sigma, Cat. # G3893, RRID:AB_477010) was validated with Western blotting by manufacturer. The rabbit anti-GFAP antibody (DAKO, Santa Clara, CA, USA, Cat. # Z0334, RRID:AB_10013382) recognizes 50 kDa protein on Western blotting from rat brain lysate (Yamanaka et al., 2011). We obtained similar staining patterns between these two antibodies and as previous studies (Yamanaka et al., 2011; Nityanandam et al., 2012).

The specificity of the mouse anti-green fluorescent protein (GFP) antibody (Millopore; Cat. # MAB3580, RRID:AB_94936) was validated by the pre-absorption experiment with GFP protein (manufacturer's information). This antibody labeled GABergic neurons in GAD67-GFP mouse sections, but no signal was detected in wild-type brain sections in the present study.

The mouse anti-HuC/D antibody (Thermo Fisher Scientific, Waltham, MA, USA; Cat. # A21271, RRID:AB_221448) label mature and immature neurons (Saito et al., 2018). The specificity of the mouse anti-HuC/D antibody was confirmed by blocking peptide with the HuD peptide (Marusich et al., 1994). With this antibody, we obtained a similar staining pattern as previous studies (Graus and Ferrer, 1990; Marusich et al., 1994).

Both the goat anti-ionized calcium-binding adaptor protein 1 (Iba1)

antibody (Abcam, Cambridge, UK, Cat. # ab5076, RRID: AB_2224402) and the rabbit anti-Iba1 antibody (Wako, Osaka, Japan, Cat. # 019-19741, RRID:AB_839504) recognize a single band at 17 kDa on Western blotting from rat brain lysate (manufacturer's information). We obtained similar staining patterns between these two antibodies and as previous studies (Hirasawa et al., 2005).

The rabbit monoclonal NeuN antibody (Abcam; Cat. # ab177487, RRID:AB_2532109) detects two bands in the 46–50kDa on Western blotting of mouse brain lysate (manufacturer's information). This antibody labels the majority of mature neurons, and we obtained a similar staining pattern as a previous study (Mullen et al., 1992).

Both the goat anti-SRY-related HMG-box 2 (Sox2) antibody (Santa Cruz, Cat. # sc17320, RRID:AB_2286684) and the rabbit anti-Sox2 antibody (Millipore; Cat. # AB5603, RRID:AB_2286686) recognize a single band at 34 kDa on Western blotting of human and mouse cell lysate (manufacturer's information). We obtained similar staining patterns between these two antibodies and as previous studies (Lagace et al., 2007).

Immunohistochemistry

The sections were incubated with primary antibodies diluted in PBS containing 0.3% Triton X-100 (0.3% PBST), overnight at 4°C. Primary antibodies were detected using species-specific donkey secondary antibodies conjugated fluorescent dyes listed in Table 2. Before the mouse-raised primary antibodies were reacted with embryonic sections, endogenous immunoglobulins were blocked with donkey anti-mouse IgG Fab fragments (0.026 mg/ml in 5% normal donkey serum and 0.3% PBST, Jackson

ImmunoResearch, West Grove, PA, USA, Cat # 715-007-003, RRID:AB_2307338) for 2 h (Li et al., 2018). The mouse-raised primary antibodies and donkey-raised secondary antibodies were diluted with 5% normal donkey serum and 0.3% PBST. To visualize nuclei, stained sections were mounted onto glass slides using a medium containing 0.2% n-propyl gallate, 50% glycerol, 5 μg/ml Hoechst 33258, and PBS.

Fluoro-Jade C staining

Sections attached to gelatin-coated glass slides were immersed in 1% NaOH/80% ethanol for 5 min, and sequentially rinsed 2 min in 70% ethanol, 2 min in distilled water, and incubated in 0.06% potassium permanganate/distilled water for 10 min. After rinsing in water for 2 min, they were incubated in 0.0001% FJC (Millipore)/0.1% acetic acid for 10 min. The sections were rinsed in distilled water three times for 1 min, dried at 50°C for 5 min, cleared in Hemo-D (Falma, Tokyo, Japan) for 1 min, and cover slipped with non-aqueous mounting medium (PARA mount, Falma). All the reactions and incubations were performed at room temperature.

FJC staining combined with immunostaining or TUNEL staining

Immunostaining was performed as describe above. TdT-mediated dUTP nick-end labeling (TUNEL) staining was performed using a MEBSTAIN Apoptosis TUNEL Kit III (MBL, Nagoya, Japan), according to the manufacturer's instructions, with a slight modification: biotin labeled-end terminals of fragmented DNA were detected with DyLight 549

labeled-streptavidin (1:2,000, Vector Laboratories, Burlingame, CA, USA). All of the fluorescently labeled free-floating sections were attached on gelatin-coated glass slides by drying at 50°C for 30 min. Then, FJC staining was performed with a modified protocol. Briefly, sections were rinsed in distilled water for 2 min, and immersed in 0.06% potassium permanganate/water for 5 min. Because the fluorescence signal can be attenuated by potassium permanganate pretreatment, the immersion time was halved (Schmued et al., 2005; Ehara and Ueda, 2009). Then, the sections were processed as described above.

Image acquisition

Images were acquired using an epi-fluorescence microscope (Eclipse 90i, Nikon, Tokyo, Japan) equipped with a digital camera (Wraycam-SR130M, Wraymer Microscope, Osaka, Japan). Single optical or stacked confocal microscopy images were acquired using an LSM 780 with 40× and 63× objective lens (Carl Zeiss, Oberkochen, Germany).

Results

FJC(+) cells in the normal and injured adult central nervous system

First, we detected FJC(+) cells throughout the normal adult SVZ-RMS-OB system. FJC(+) cells exhibited irregular shapes or small, circular shapes. Moreover, FJC(+) cells had pyknotic nuclei when visualized with Hoechst33258 staining (Figure 1B, C, and D). These results are consistent

with those from previous studies performed on rat sections, but the number of FJC(+) cells was fewer in our study than in previous studies (Mitrušková et al., 2005; Račeková et al., 2009). The signal intensity of FJC(+) cells in the SVZ-RMS-OB system in the normal adult brain was weaker than that in the injured adult cortex (see below). Most of the FJC(+) cells in the SVZ-RMS-OB system were also Cas3(+), a marker of apoptotic cells (Figure 1C and D, arrows). In contrast, FJC(+)/Cas3 negative (-) cells were also observed (Figure 1B, arrowheads), although the number of FJC(-)/Cas3(+) cells was low (Figure 1B, open arrowheads). In principle, few FJC(+) cells were observed outside of the SVZ-RMS-OB system (see below).

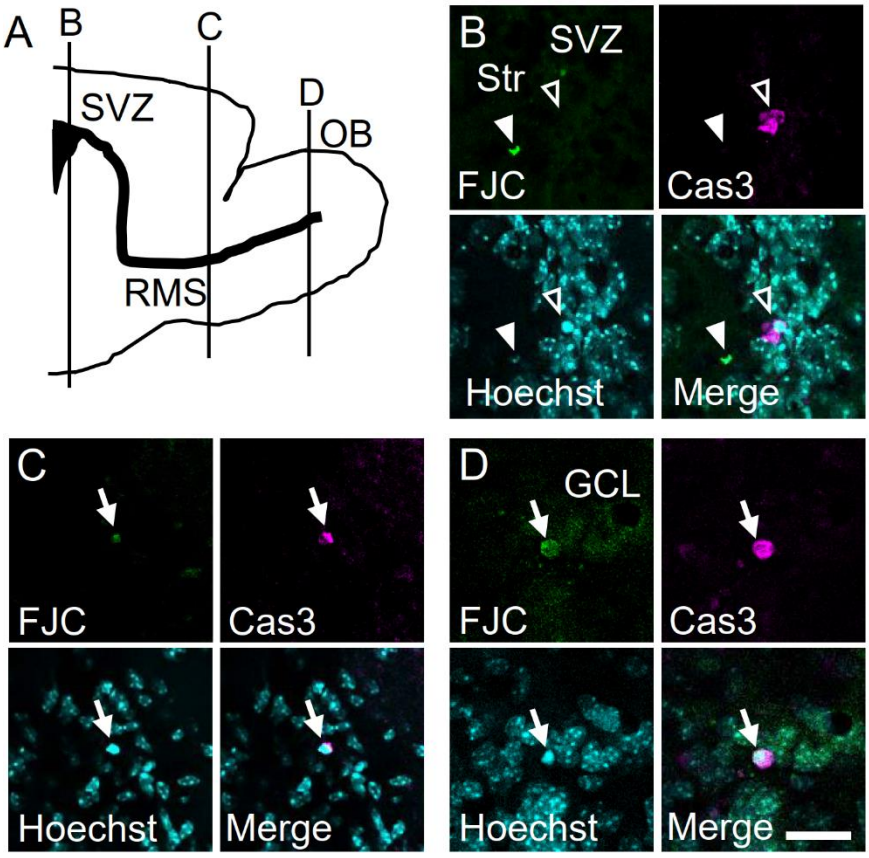

Figure 1. FJC(+) cells in the adult SVZ-RMS-OB system. (A) Schema of the SVZ-RMS-OB system in the sagittal plane. Single optical confocal

microscopy images of FJC staining, combined with Cas3 immunostaining, at the level of the SVZ (B), RMS (C), and OB (D) are shown. Virtually all of the Cas3(+) cells were FJC(+), but FJC(+)/Cas3(-) cells (arrowheads) and FJC(-)/Cas3(+) cells could be observed (open arrowheads). FJC(+) and Cas3(+) cells had pyknotic nuclei. SVZ, subventricular zone; RMS, rostral migratory stream; OB, olfactory bulb; Str, striatum, GCL, granule cell layer of the OB. Scale bar: 20 μm.

Second, we examined the cell types of the FJC(+) cells in the SVZ-RMS-OB system. To identify cell types, we performed immunostaining using FJC combined with the following markers: NeuN, a marker for mature neurons; DCX, a marker for migrating neuroblasts; GFAP, a marker for astrocytes/neural stem cells; and Iba1, a marker for microglia. We detected FJC(+)/DCX(+) cells in the RMS/OB (Figure 2A and B), in addition to FJC(+)/NeuN(+) cells in the OB (Figure 2C). A very small number of FJC(+)/GFAP(+) cells were observed in the RMS (Figure 3A, arrows), and their processes were visualized by FJC (Figure 3A', arrowheads). Moreover, we detected apoptotic GFAP(+) astrocytes in the RMS (Figure 3B, arrows). In addition, FJC(+)/Iba1(+) cells (Figure 3C, arrows) and Cas3(+)/Iba1(+) cells with pyknotic nuclei in the RMS/OB (data not shown) were observed, and a much smaller number of these cells were also detected outside of the SVZ-RMS-OB system (data not shown). These results suggest that some FJC(+) cells may represent degenerating microglia or degenerating cells being engulfed by microglia. To discriminate between these possibilities, we analyzed GAD67-GFP mice. In the SVZ-RMS-OB system, DCX(+) cells express GAD67, a rate-limiting enzyme involved in GABA synthesis, and

GAD67-GFP mice express green fluorescent protein (GFP) under the control of GAD67 promoter (Tamamaki et al., 2003; Saito et al., 2018). In principle, Iba1(+) microglia were GFP(-) (Figure 3D, open arrowheads). Both Cas3(+)/Iba1(+)/GFP(+) cells (Figure 3D, arrows) and Cas3(+)/Iba1(+)/GFP(-) cells (Figure 3E, arrowheads) were observed in the RMS/OB.

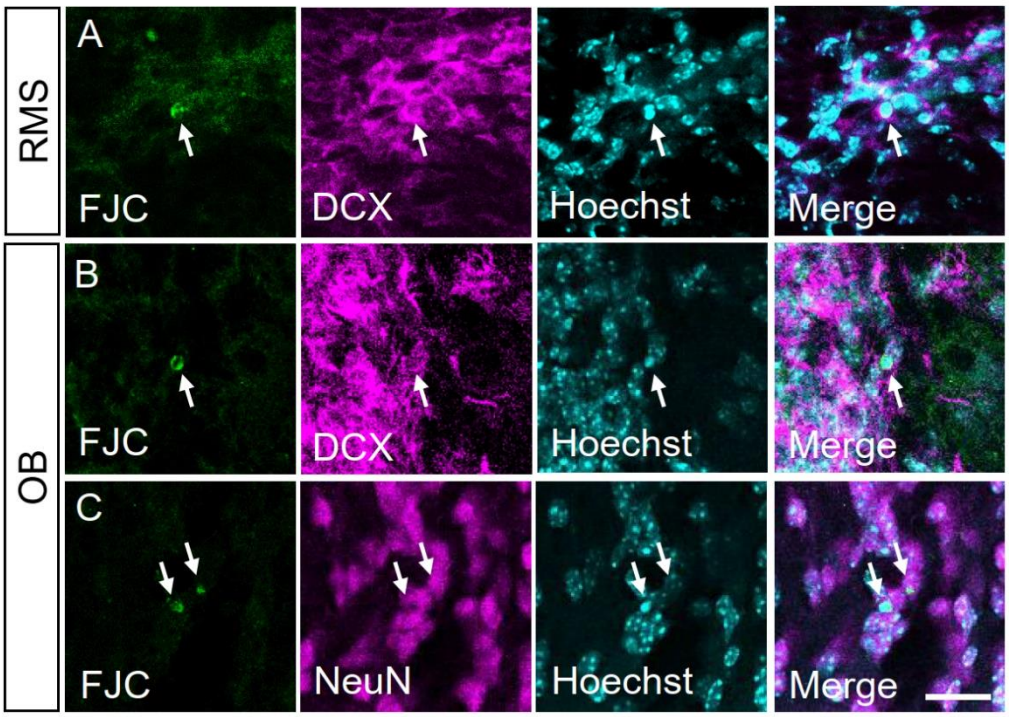

Figure 2. Identification of FJC(+) cells in the SVZ-RMS-OB system. FJC(+) cells were DCX(+) neuroblasts in the RMS (A) and OB (B), or NeuN(+) mature neurons in the OB (C). Single optical confocal microscopy images are shown. Arrows indicate the double (+) cells. Scale bar: 20 μm.

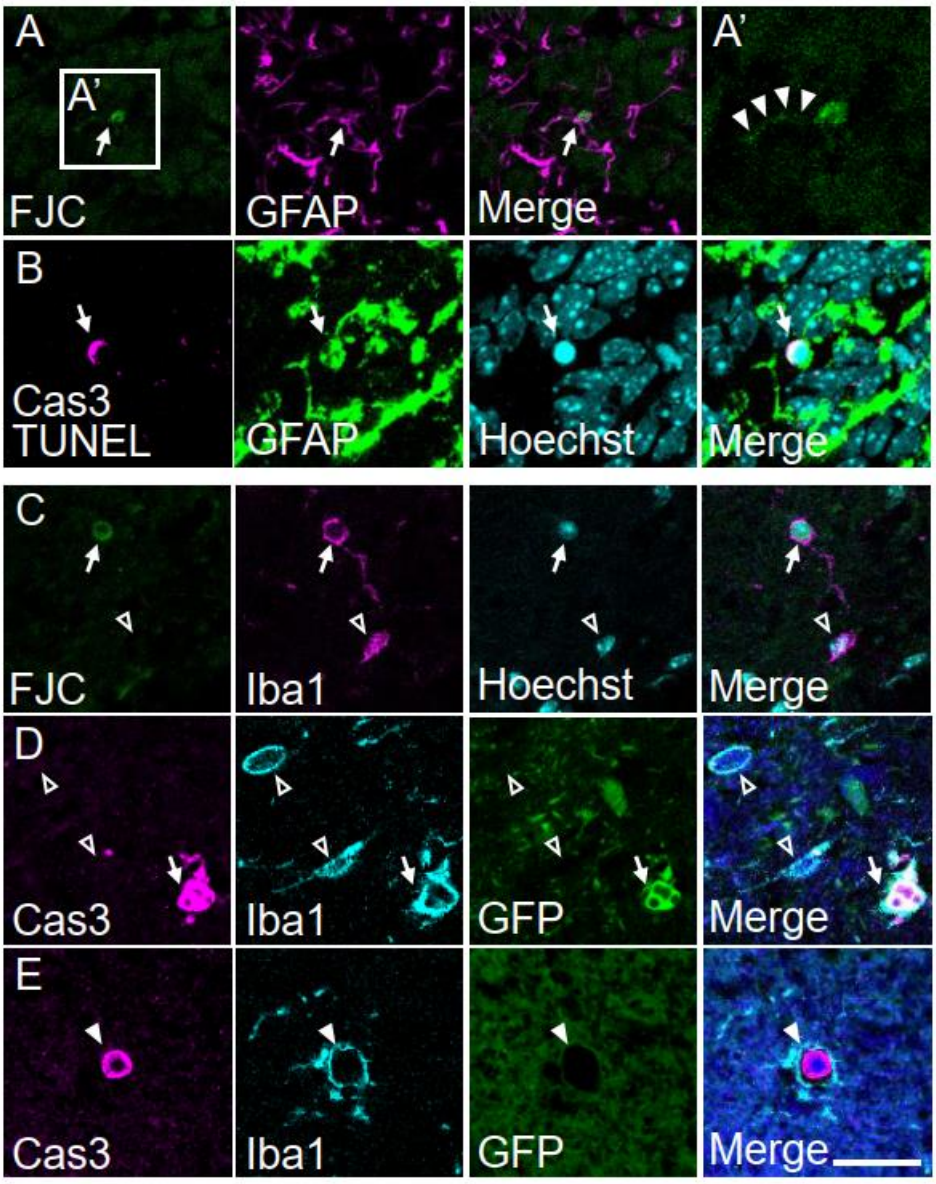

Figure 3. FJC(+) glial cells in the normal adult SVZ-RMS-OB system. (A) An FJC(+)/GFAP(+) cell with an FJC(+) process in the RMS. (A') A high magnification image of the box in (A). (B) An apoptotic GFAP(+) astrocyte in the RMS. Apoptotic cells (Cas3(+) and/or TUNEL(+)) were labeled in magenta, and GFAP(+) astrocytes were labeled in green. (C) An FJC(+)/Iba1(+) cell in the OB. A Cas3(+)/Iba1(+)/GFP(+) cell (D, arrows) and a Cas3(+)/Iba1(+)/GFP(-) cell (E, arrowheads) in the OB of GAD67-GFP mouse. Iba1(+) microglia were GFP(-) (D, open arrowheads). Merged images of (D) and (E) include Hoechst33258 images. Single optical (A, C-E) and

stacked (B) confocal microscopy images are shown. Scale bar: 10 μm for A', 20 μm for A-E.

Third, we detected many FJC(+) cells close to the damaged area of the adult cerebral cortex 1 day after stab injury, but the number of FJC(+) cells decreased 4 days after injury (data not shown). The signal intensity of these FJC(+) cells was much higher than in the normal SVZ-RMS-OB system, and their processes were clearly detected (data not shown). Judging from their morphology, those cells with intense FJC signal should be neurons. There were neither FJC(+)/GFAP(+) cells nor FJC(+)/Iba1(+) cells close to the injured site (data not shown). In the normal adult spinal cord, GFAP(+) and Iba1(+) cells were FJC(-) (data not shown).

FJC(+) cells in the E14 embryonic cortex

Next, we examined the embryonic brain to determine whether FJC staining can detect proliferating neural stem/precursor cells. No FJC(+) cells and Cas3(+) cells were detected in the normal E14 brain (Figure 4A and C). To facilitate analysis, we induced apoptosis in neural stem/precursor cells by injecting ENU (William et al., 2004; Katayama et al., 2005). In the ENU-treated E14 embryonic cortex, FJC(+)/Cas3(+) cells and FJC(+)/TUNEL(+) cells were scattered throughout the ventricular/subventricular zone (VZ/SVZ) and mantle layer (ML) of the cerebral cortex (Figure 4B and D-I). FJC(+) cells exhibited a rounded shape, but did not show processes. Virtually all of the Cas3(+) or TUNEL(+) cells were FJC(+) (Figure 4E, F, H, and I, arrows), but a considerable number of

FJC(+)/Cas3(-) cells and FJC(+)/TUNEL(-) cells were observed (Figure 4E, F, H, and I, arrowheads).

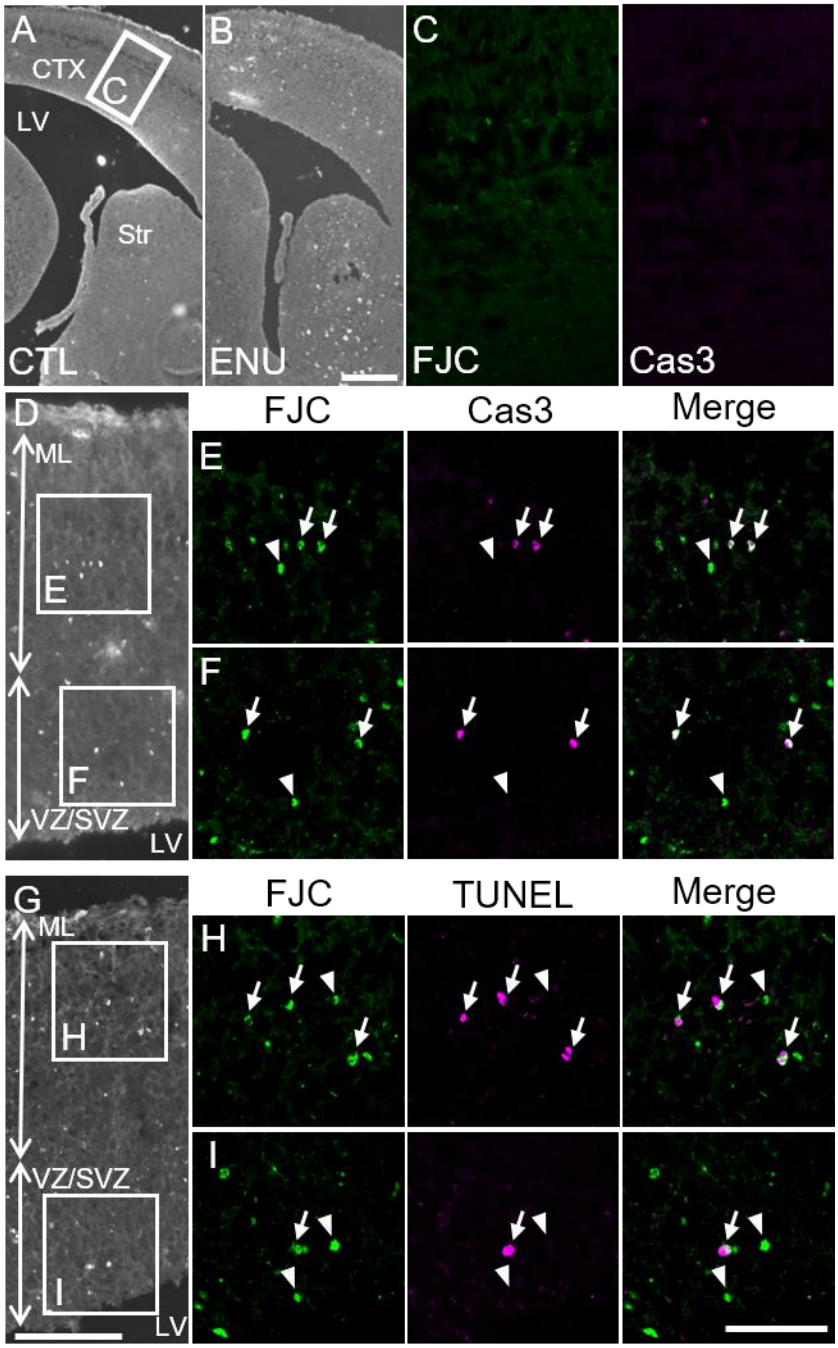

Figure 4. FJC(+) degenerating cells in the ENU-treated-E14 embryonic brain. (A) There were no FJC(+) cells in the control brain. (B and D-I) Many FJC(+) cells were detected throughout the brain of the ENU treated embryo. (C) High magnification images of the boxed area in (A) are shown. In the

control brain, neither FJC(+) nor Cas3(+) cells were detected. (D-F) Virtually all of the Cas3(+) cells were FJC(+) (arrows) in the ML (E) and VZ/SVZ (F), but FJC(+)/Cas3(-) cells were also detected (arrowheads). High magnification images of the boxed area in (D) are shown. (G-I) Virtually all of the TUNEL(+) cell were FJC(+) in the ML (H) and VZ/SVZ (I) (arrows), but FJC(+)/TUNEL(-) cells were also detected (arrowheads). Low and high magnification images were obtained using an epi-fluorescence microscopy and a confocal microscopy (single optical sections), respectively. CTX, cortex; LV, lateral ventricle; ML, mantle layers; VZ/SVZ, ventricular zone and subventricular zone. Scale bars: 200 μm in B for A and B; 100 μm in G for D and G; and 50 μm in I for C, E, F, H, and I.

Neural stem/precursor cells and postmitotic young neurons reside in the embryonic VZ/SVZ and ML, respectively (Noctor et al., 2002). Thus, we identified the cell types of FJC(+) cells in the ENU-treated embryonic cortex by using markers for neural stem/precursor cells (Sox2), postmitotic migrating neurons (DCX), and differentiated neurons (HuC/D). In general, the fluorescent immunostaining signal fades during the processing necessary for FJC staining, especially during the potassium permanganate pretreatment (Schmued et al., 2005; Ehara and Ueda, 2009). In addition, the immunostaining signals for Sox2, DCX, and HuC/D were relatively weaker than those for Cas3 and TUNEL. Thus, it was difficult to acquire clear images of FJC(+)/Sox2(+), FJC(+)/DCX(+), and FJC(+)/HuC/D(+) cells. To overcome this issue, we took advantage of the result that virtually all Cas3(+) cells were FJC(+), as described above. In the ENU-treated E14

embryonic cortex, Cas3(+)/Sox2(+), Cas3(+)/DCX(+), and Cas3(+)/HuC/D(+) cells were detected (Figure 5A-F).

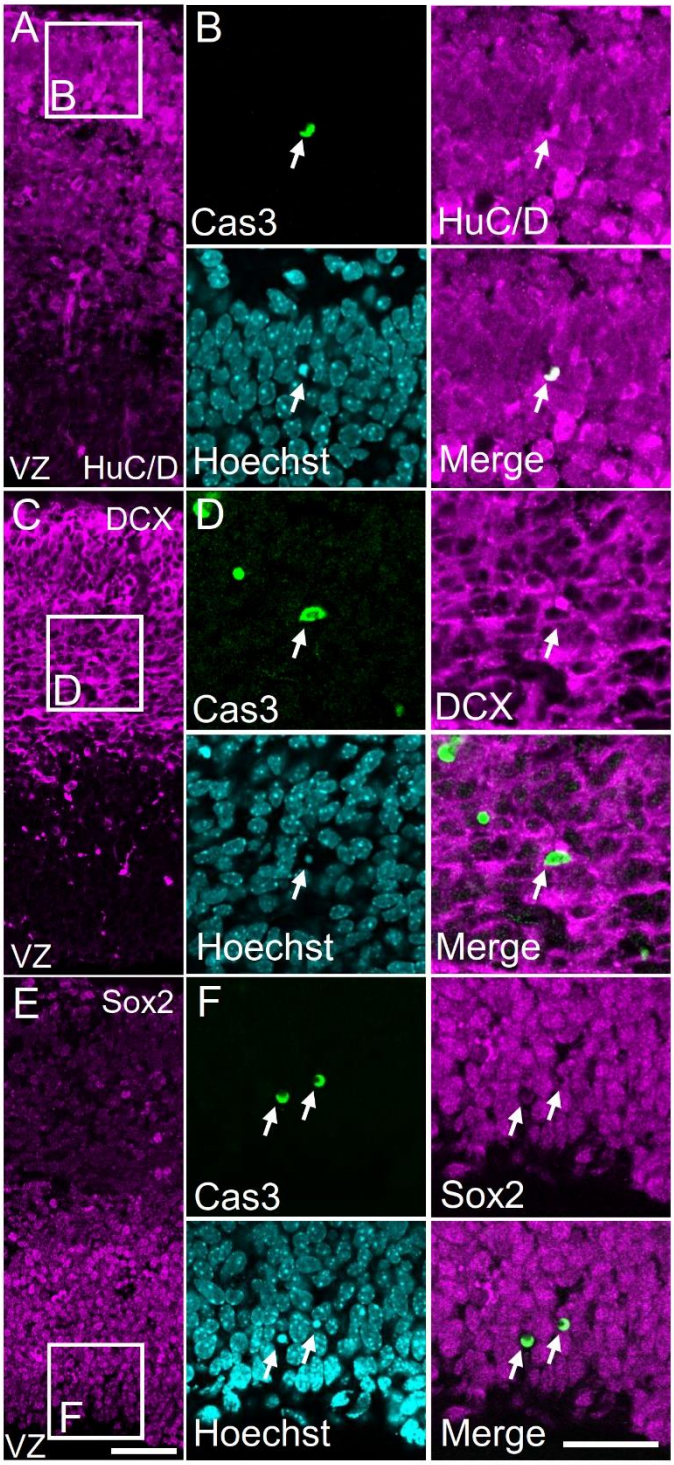

Figure 5. Identification of Cas3(+) apoptotic cells in the ENU-treated E14 embryonic brain. Cas3(+) cells were HuC/D(+) differentiated neurons in the ML (A and B), DCX(+) postmitotic migrating neurons in the ML (C and D), and Sox2(+) neural stem/precursor cells in the VZ/SVZ (E and F). Single optical confocal microscopy images are shown. Scale bars: 50 μm in E for A, C, and E; 50 μm in F for B, D and F.

FJC(+)/Cas3(+) cells in the E10 embryo

Before the neurogenic period during development, the neural stem cell pool enlarges through the symmetrical division of neuroepithelial cells until approximately E10 (Götz and Huttner, 2005; Jiang and Nardelli, 2015). At this stage, ethanol injections into pregnant mice can induce massive apoptosis throughout the embryonic body (Dunty et al., 2001). In the control E10 embryonic brain, FJC(+) cells were not detected (Figure 6A). In contrast, in ethanol-treated E10 embryos, a considerable number of FJC(+) cells were detected (Figure 6B). Almost all of the Cas3(+) cells were FJC(+) (Figure 6C, arrows), but FJC(+)/Cas3(-) cells were also detected (Figure 6C, arrowheads). FJC(+) cells with pyknotic nuclei in the presumptive central nervous system were Sox2(+) neuroepithelial cells (Figure 6D, arrows). FJC(+)/Cas3(+) cells (data not shown) and FJC(+)/Sox2(-) cells were also present outside of the presumptive central nervous system (Figure 6D, arrowheads). Those FJC(+) cells were not migrating neural crest cells, because they did not express DCX (data not shown) (Vermillion et al., 2014). FJC(+) cells had strong signals in these sections, showing rounded or irregular morphology, without processes (Figure 6C and D).

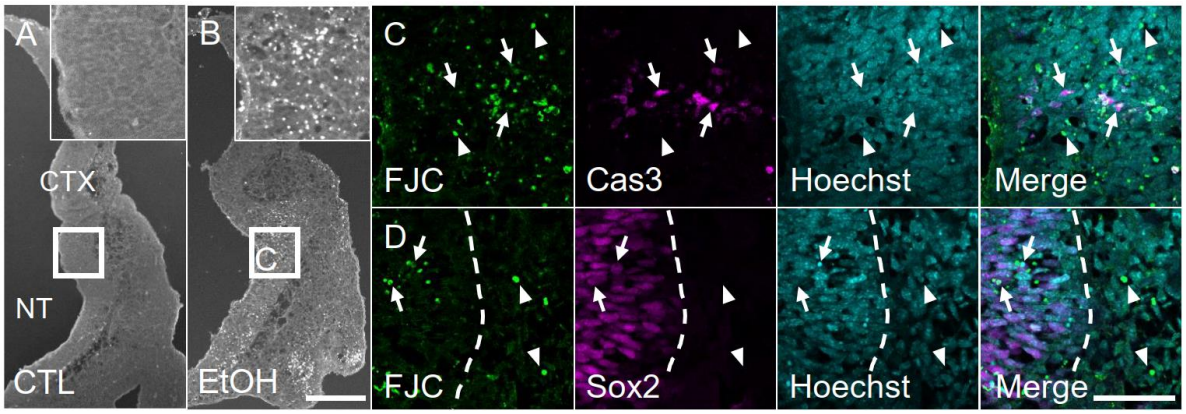

Figure 6. FJC(+) degenerating cells in the ethanol-treated E10 embryo. (A) No FJC(+) cells were detected in the control embryo. (B) In contrast, a lot of FJC(+) cells were detected in the ethanol-treated E10 embryonic brain. (C) High magnification images of the boxed area in (B) are shown. Almost all of the Cas3(+) cells were FJC(+) (arrows). FJC(+)/Cas3(-) cells were also detected (arrowheads). (D) The border between the neural tissue (spinal cord) and the mesenchymal tissues in the ethanol-treated embryo is shown. FJC(+)/Sox2(+) neuroepithelial cells were detected in the spinal cord (arrows), and FJC(+)/Sox2(-) cells were detected in the mesenchyme (arrowheads). Epi-fluorescence microscopy images (A and B) and single optical confocal microscopy images (C and D) are shown. NT, neural tube. Scale bars: 200 μm in B for A and B; 50 μm in D for C and D.

Discussion

In this study, we focused on the validity of FJC staining for the detection of degenerating neuronal cells in adult and embryonic brains. To identify the cell types of FJC(+) cells, we performed FJC staining combined with immunostaining. In addition, we reexamined the specificity of FJC staining for degenerating neuronal cells.

FJC can detect degenerating immature neurons in the normal adult brain

In the adult rodent SVZ-RMS-OB system, new neurons are produced throughout life. During this process, approximately half of the immature neuronal cells are eliminated through apoptosis (Biebl et al., 2000). Although previous studies revealed that FJB(+) and FJC(+) cells exist in this region, the cell types of those FJs(+) cells remained unclear (Mitrušková et al., 2005; Račeková et al., 2009). We also detected FJC(+) cells throughout the SVZ-RMS-OB system, but the number of FJC(+) cells was much smaller in our study than in previous studies. This difference might be due to differences in the animal species used in the different studies (mouse or rat). We revealed that FJC(+) cells were not only NeuN(+) mature neurons in the OB, but also DCX(+) neuroblasts in the RMS/OB. These results clearly indicate that FJC staining can detect immature neurons in the adult brain.

A small number of FJC(-)/Cas3(+) apoptotic cells were observed in the normal adult SVZ-RMS-OB system. This result indicates that not all of the degenerating mature/immature neurons can be detected by FJC staining (He et al., 2005; Chidlow et al., 2009). Moreover, FJC staining can usually visualize the processes of degenerating neurons in the injured adult brain, but the FJC(+)/NeuN(+) cells and FJC(+)/DCX(+) cells in the normal SVZ-RMS-OB system rarely exhibited FJC(+) processes. These issues might be the result of the much weaker FJC signal detected in the normal brain compared with the injured brain. In addition, we could not detect FJC(+) cell processes for injured embryonic neuronal cells (see below). Thus, there could be some differences between normal and injured conditions in the adult brain with regards to the molecular structures of degenerating neuronal

cells that interact with FJC, in addition to differences between the adult and embryonic injured brain.

FJC can detect degenerating neural stem/precursor cells in the embryonic brain

Our results in the adult brain prompted us to examine whether FJC staining can detect the degeneration of neural stem/precursor cells. In the embryonic mouse brain, neurogenesis begins at approximately E11, and neurons are massively produced starting at approximately E14 (Caviness, 1982). Before the neurogenic period, neuroepithelial cells divide symmetrically to enlarge the neural stem cell pool (Götz and Huttner, 2005; Jiang and Nardelli, 2015). During neurogenic periods, Sox2(+) neural stem/precursor cells reside in the VZ/SVZ, and they proliferate through symmetrical or asymmetric division to generate sister neural stem cells, secondary neural precursor cells, or postmitotic neurons (Miyata et al., 2001; Tamamaki et al., 2001; Noctor et al., 2002; Götz and Huttner, 2005; Bani-yaghoub et al., 2006). DCX(+) postmitotic cells migrate out from the VZ/SVZ, and HuC/D(+) differentiated neurons locate in the ML (Okano and Darnell, 1997; Francis et al., 1999).

In the present study, we showed that virtually all of the Cas3(+) or TUNEL(+) cells were FJC(+), and Cas3(+) cells were Sox2(+), DCX(+), or HuC/D(+) cells in the ENU-treated E14 embryonic cortex. Moreover, we detected FJC(+) neuroepithelial cells in the ethanol-treated E10 embryonic neural tissue. These results indicate that FJC staining can detect degenerating neuronal cells at all differentiation stages, including neuroepithelial cells, neural stem/precursor cells, immature neurons, and mature neurons.

Is FJC staining specific to degenerating neuronal cells?

During the apoptotic process, the activation (cleaving) of Caspase 3 is a relatively early step, and DNA fragmentation (detected by TUNEL staining) is a late step (Susan, 2007). In the ENU- and ethanol-treated embryos, both FJC(+)/Cas3(+) and FJC(+)/TUNEL (+) cells were detected. These results indicate that FJC staining can detect apoptotic cells from early to late stages. Thus, FJC(+)/Cas3(-) and FJC(+)/TUNEL(-) cells might be FJC(+)/TUNEL(+) and FJC(+)/Cas3(+) cells, respectively.

Although there are some conflicting data (Colombo and Puissant, 2002; Anderson et al., 2003; Damjanac et al., 2007; Chidlow et al., 2009; Ehara and Ueda, 2009), FJs are generally considered to be specific to degenerating neurons. In principle, our results examining the stab-injured adult cortex and normal adult spinal cords support this notion; however, we detected a small number of FJC(+)/Iba1(+) cells and Cas3(+)/Iba1(+) cells with pyknotic nuclei in the normal adult RMS/OB and cerebral cortex. Triple immunostaining with Cas3, Iba1, and GFP (expressed in GAD67-GFP knock-in mice) revealed that both Cas3(+)/Iba1(+)/GFP(+) cells and Cas3(+)/Iba1(+)/GFP(-) cells were present. In the GAD67-GFP mice, DCX(+) neuroblasts and mature/immature GABAergic neurons in the SVZ-RMS-OB system were GFP(+) (Saito et al., 2018), but microglia were GFP(-) (Tamamaki et al., 2003). Thus, Cas3(+)/Iba1(+)/GFP(+) cells might represent microglia engulfing degenerating GFP(+) cells. In contrast, Cas3(+)/Iba1(+)/GFP(-) cells might represent GFP(-) degenerating cells phagocytosed by microglia or degenerating microglia.

In addition, we detected a few FJC(+)/GFAP(+) cells in the RMS and OB.

Our results in the embryonic brain indicate that FJC can detect degenerating neural stem cells. In fact, GFAP(+) Type-B cells (adult neural stem cells) also reside in the RMS (Nityanandam et al., 2012). Thus FJC(+)/GFAP(+) cells in the RMS could represent degenerating Type-B cells. However, the majority of GFAP(+) cells in the RMS should represent the astrocytes that form the glial tube sheathing migrating neuroblasts. They could correspond to FJC(+) "quiescent" astrocytes as Anderson et al described (Anderson et al., 2003). Unfortunately, there is no strict marker to discriminate between GFAP(+) neural stem cells and GFAP(+) astrocytes. Alternatively, those FJC(+)/GFAP(+) cells could be false positive cells with faint FJC signal as described previously (Schmued et al., 2005; Brown and Sawchenko, 2007; Chidlow et al., 2009). But it is unlikely, because we found a few Cas3(+)/TUNEL(+)/GFAP(+) cells in the RMS/OB. Further studies are needed to clear these issues.

Outside of the nervous system, Cas3(+) degenerating mesenchymal cells with pyknotic nuclei became FJC(+) in the ethanol-treated embryo. Although FJB can stain dying tubular cells of the kidney (Ikeda et al., 2017), our study represents the first report that FJC stains degenerating non-neural cells.

In conclusion, the present study indicates that FJC staining can detect degenerating neuronal cells including mature neurons, immature neurons, neural stem/precursor cells, and neuroepithelial cells. Even though FJC signal is fainter under normal condition, FJC staining can be useful for the detection of degenerating neuronal cells. However, we must consider that there could be small number of degenerating astrocytes and microglia that result in a faint positive FJC signal in the normal brain.

Declaration of conflicting interests

The authors declare no potential conflicts of interest with respect to the research, authorship, and /or publication of this article.

Author's contributions

TI, HK, and TS conducted the experiments and analyzed the data; YH critically revised the results and manuscript; TM designed and supervised the study.

Acknowledgement

This research was partly performed at the Tottori Bio Frontier, managed by the Tottori prefecture.

Funding

This work was supported by JSPS KAKENHI [Grant Numbers JP17K16264 and JP18K06830].

References

Altman J (1969) Autoradiographic and histological studies of postnatal neurogenesis. J Comp Neurol 137:433–457 DOI: 10.1002/cne.901370404.

Anderson KJ, Fugaccia I, Scheff SW (2003) Fluoro-jade B stains quiescent and reactive astrocytes in the rodent spinal cord. J Neurotrauma 20:1223–1231 DOI: 10.1089/089771503770802899.

Azevedo PO, Lousado L, Paiva AE, Andreotti JP, Santos GSP, Sena IFG, Prazeres PHDM, Filev R, Mintz A, Birbrair A (2017) Endothelial cells maintain neural stem cells quiescent in their niche. Neuroscience 363:62–65 DOI: 10.1016/j.neuroscience.2017.08.059.

Ballok DA, Millward JM, Sakic B (2003) Neurodegeneration in autoimmune MRL-lpr mice as revealed by Fluoro Jade B staining. Brain Res 964:200–210 DOI: 10.1016/j.brainres.2007.07.089.

Bani-yaghoub M, Tremblay RG, Lei JX, Zhang D, Zurakowski B, Sandhu JK, Smith B, Ribecco-Lutkiewicz M, Kennedy J, Walker PR, Sikorska M (2006) Role of Sox2 in the development of the mouse neocortex. Dev Biol 295:52–66 DOI: 10.1016/j.ydbio.2006.03.007.

Biebl M, Cooper CM, Winkler È, Kuhn HG (2000) Analysis of neurogenesis and programmed cell death reveals a self- renewing capacity in the adult rat brain. 291:3–6.

Brandt MD, Jessberger S, Steiner B, Kronenberg G, Reuter K, Bick-Sander A, von der Behrens W, Kempermann G, Behrens W Von Der, Kempermann G (2003) Transient calretinin expression defines early postmitotic step of neuronal differentiation in adult hippocampal neurogenesis of mice. Mol Cell Neurosci 24:603–613 DOI:

10.1016/S1044-7431(03)00207-0.

Brown DA, Sawchenko PE (2007) Time course and distribution of inflammatory and neurodegenerative events suggest structural bases for the pathogenesis of experimental autoimmune encephalomyelitis. J Comp Neurol 502:236–260 DOI: 10.1002/cne.21307.

Cammermeyer J (1961) The importance of avoiding “dark” neurons in experimental neuropathology. Acta Neuropathol 1:245–270 DOI: 10.1007/BF00687191.

Caviness VS (1982) Neocortical histogenesis in normal and reeler mice: A developmental study based upon [3H]thymidine autoradiography. Dev Brain Res 4:293–302 DOI: 10.1016/0165-3806(82)90141-9.

Chidlow G, Wood JP, Sarvestani G, Manavis J, Casson RJ (2009) Evaluation of Fluoro-Jade C as a marker of degenerating neurons in the rat retina and optic nerve. Exp Eye Res 88:426–437 DOI: 10.1016/j.exer.2008.10.015.

Colombo JA, Puissant VI (2002) Fluoro Jade stains early and reactive astroglia in the primate cerebral cortex. J Histochem Cytochem 50:1135–1137 DOI: 10.1177/002215540205000815.

Damjanac M, Bilan AR, Barrier L, Pontcharraud R, Anne C, Hugon J, Page G (2007) Fluoro-Jade® B staining as useful tool to identify activated microglia and astrocytes in a mouse transgenic model of Alzheimer’s disease. Brain Res 1128:40–49 DOI: 10.1016/j.brainres.2006.05.050.

Doetsch F, García-Verdugo JM, Alvarez-Buylla A (1997) Cellular composition and three-dimensional organization of the subventricular germinal zone in the adult mammalian brain. J Neurosci 17:5046–5061 DOI: 10.1002/CNE.902890106.

Dunty WC, Chen S, Zucker RM, Dehart DB, Sulik KK (2001) Selective Vulnerability of Embryonic Cell Populations to Ethanol-Induced Apoptosis : Implications for Alcohol- Related Birth Defects and Neurodevelopmental Disorder. 25:1523–1535.

Ehara A, Ueda S (2009) Application of Fluoro-Jade C in Acute and Chronic Neurodegeneration Models: Utilities and Staining Differences. Acta Histochem Cytochem 42:171–179 DOI: 10.1267/ahc.09018.

Fernandes AMAP, Maurer-Morelli C V., Campos CBL, Mello MLS, Castilho RF, Langone F (2004) Fluoro-Jade, but not Fluoro-Jade B, stains non-degenerating cells in brain and retina of embryonic and neonatal rats. Brain Res 1029:24–33 DOI: 10.1016/j.brainres.2004.09.036.

Francis F, Koulakoff A, Boucher D, Chafey P, Schaar B, Vinet MC, Friocourt G, McDonnell N, Reiner O, Kahn A, McConnell SK, Berwald-Netter Y, Denoulet P, Chelly J (1999) Doublecortin is a developmentally regulated, microtubule-associated protein expressed in migrating and differentiating neurons. Neuron 23:247–256 DOI: 10.1016/S0896-6273(00)80777-1.

Goodyear RJ, Ratnayaka HSK, Warchol ME, Richardson GP (2014) Staurosporine-induced collapse of cochlear hair bundles. J Comp Neurol 522:3281–3294 DOI: 10.1002/cne.23597.

Götz M, Huttner WB (2005) The cell biology of neurogenesis. Nat Rev Mol Cell Biol 6:777–788 DOI: 10.1038/nrm1739.

Graus F, Ferrer I (1990) Analysis of a neuronal antigen (Hu) expression in the developing rat brain detected by autoantibodies from patients with paraneoplastic encephalomyelitis. Neurosci Lett 112:14–18 DOI: 10.1016/0304-3940(90)90314-y.

Gu Q, Lantz-McPeak S, Rosas-Hernandez H, Cuevas E, Ali SF, Paule MG, Sarkar S (2014) In vitro detection of cytotoxicity using FluoroJade-C. Toxicol In Vitro 28:469–472 DOI: 10.1016/j.tiv.2014.01.007.

He Z, Crook JE, Meschia JF, Brott TG, Dickson DW, McKinney M (2005) Aging blunts ischemic-preconditioning-induced neuroprotection following transient global ischemia in rats. Curr Neurovasc Res 2:365–374 DOI: 10.2174/156720205774962674.

Hirasawa T, Ohsawa K, Imai Y, Ondo Y, Akazawa C, Uchino S, Kohsaka S (2005) Visualization of microglia in living tissues using Iba1-EGFP transgenic mice. J Neurosci Res 81:357–362 DOI: 10.1002/jnr.20480.

Ikeda M, Wakasaki R, Schenning KJ, Swide T, Lee JH, Miller MB, Choi HS, Anderson S, Hutchens MP (2017) Determination of renal function and injury using near-infrared fluorimetry in experimental cardiorenal syndrome. Am J Physiol Renal Physiol 312:F629–F639 DOI: 10.1152/ajprenal.00573.2016.

Ishida K, Shimizu H, Hida H, Urakawa S, Ida K, Nishino H (2004) Argyrophilic dark neurons represent various states of neuronal damage in brain insults: some come to die and others survive. Neuroscience 125:633–644 DOI: 10.1016/j.neuroscience.2004.02.002.

Jankovski A, Sotelo C (1996) Subventricular zone-olfactory bulb migratory pathway in the adult mouse: Cellular composition and specificity as determined by heterochronic and heterotopic transplantation. J Comp Neurol 371:376–396 DOI: 10.1002/(SICI)1096-9861(19960729)371:3<376::AID-CNE3>3.3.CO;2-V.

Jiang X, Nardelli J (2015) Cellular and molecular introduction to brain development. Neurobiol Dis 92:3–17 DOI: 10.1016/j.nbd.2015.07.007.

Katayama K, Ueno M, Yamauchi H, Nagata T, Nakayama H, Doi K (2005) Ethylnitrosourea induces neural progenitor cell apoptosis after S-phase accumulation in a p53-dependent manner. Neurobiol Dis 18:218–225 DOI: 10.1016/j.nbd.2004.09.015.

Knapp L, Gellért L, Herédi J, Kocsis K, Oláh G, Fuzik J, Kis Z, Vécsei L, Toldi J, Farkas T (2014) A simple novel technique to induce short-lasting local brain ischaemia in the rat. Neuropathol Appl Neurobiol 40:603–609 DOI: 10.1111/nan.12069.

Krinke GJ, Classen W, Vidotto N, Suter E, Würmlin C (2001) Detecting necrotic neurons with fluoro-jade stain. Exp Toxicol Pathol 53:365–372 DOI: 10.1078/0940-2993-00202.

Lagace DC, Whitman MC, Noonan MA, Ables JL, Decarolis NA, Arguello AA, Donovan MH, Fischer SJ, Farnbauch LA, Beech RD, Dileone RJ, Greer CA, Mandyam CD, Eisch AJ (2007) Dynamic Contribution of Nestin-Expressing Stem Cells to Adult Neurogenesis. 27:12623–12629 DOI: 10.1523/JNEUROSCI.3812-07.2007.

Leonard JR, D'Sa C, Klocke BJ, Roth KA (2001) Neural precursor cell apoptosis and glial tumorigenesis following transplacental ethyl-nitrosourea exposure. Oncogene 20:8281–8286 DOI: 10.1038/sj.onc.1205024.

Li Y, Viscidi RP, Kannan G, McFarland R, Pletnikov M V., Severance EG, Yolken RH, Xiao J, Xiaoa J (2018) Chronic Toxoplasma gondii Infection Induces Anti- N -Methyl-D-Aspartate Receptor Autoantibodies and Associated Behavioral Changes and Neuropathology. Infect Immun 86:1–12 DOI: 10.1128/IAI.00398-18.

Lois C, Alvarez-Buylla A (1994) Long-distance neuronal migration in the

adult mammalian brain. Science 264:1145–1148 DOI: 10.1126/science.8178174.

Marusich MF, Furneaux HM, Henion PD, Weston JA (1994) Hu neuronal proteins are expressed in proliferating neurogenic cells. J Neurobiol 25:143–155 DOI: 10.1002/neu.480250206.

Mitrušková B, Orendáčová J, Račeková E (2005) Fluoro Jade-B detection of dying cells in the SVZ and RMS of adult rats after bilateral olfactory bulbectomy. Cell Mol Neurobiol 25:1255–1263 DOI: 10.1007/s10571-005-8502-1.

Miyata T, Kawaguchi A, Okano H, Ogawa M (2001) Asymmetric inheritance of radial glial fibers by cortical neurons. Neuron 31:727–741 DOI: 10.1016/S0896-6273(01)00420-2.

Mullen RJ, Buck CR, Smith AM (1992) NeuN , a neuronal specific nuclear protein in vertebrates. 211:201–211.

Nityanandam A, Parthasarathy S, Tarabykin V (2012) Postnatal subventricular zone of the neocortex contributes GFAP+ cells to the rostral migratory stream under the control of Sip1. Dev Biol 366:341–356 DOI: 10.1016/j.ydbio.2012.03.013.

Noctor SC, Flint AC, Weissman TA, Wong WS, Clinton BK, Kriegstein AR (2002) Dividing precursor cells of the embryonic cortical ventricular zone have morphological and molecular characteristics of radial glia. J Neurosci 22:3161–3173 DOI: 20026299.

Okano HJ, Darnell RB (1997) A hierarchy of Hu RNA binding proteins in developing and adult neurons. J Neurosci 17:3024–3037.

Račeková E, Lievajová K, Danko J, Martončíková M, Flešárová S, Almašiová V, Orendáčová J (2009) Maternal separation induced alterations of

neurogenesis in the rat rostral migratory stream. Cell Mol Neurobiol 29:811–819 DOI: 10.1007/s10571-009-9362-x.

Ribeiro Xavier AL, Kress BT, Goldman SA, Lacerda de Menezes JR, Nedergaard M (2015) A Distinct Population of Microglia Supports Adult Neurogenesis in the Subventricular Zone. J Neurosci 35:11848–11861 DOI: 10.1523/JNEUROSCI.1217-15.2015.

Saito K, Koike T, Kawashima F, Kurata H, Shibuya T, Satoh T, Hata Y, Yamada H, Mori T (2018) Identification of NeuN immunopositive cells in the adult mouse subventricular zone. J Comp Neurol 526:1927–1942 DOI: 10.1002/cne.24463.

Schmued LC, Albertson C, Slikker W (1997) Fluoro-Jade: A novel fluorochrome for the sensitive and reliable histochemical localization of neuronal degeneration. Brain Res 751:37–46 DOI: 10.1016/S0006-8993(96)01387-X.

Schmued LC, Hopkins KJ (2000) Fluoro-Jade B: A high affinity fluorescent marker for the localization of neuronal degeneration. Brain Res 874:123–130 DOI: 10.1016/S0006-8993(00)02513-0.

Schmued LC, Stowers CC, Scallet AC, Xu L (2005) Fluoro-Jade C results in ultra high resolution and contrast labeling of degenerating neurons. Brain Res 1035:24–31 DOI: 10.1016/j.brainres.2004.11.054.

Shi M, Wang Y-Q, Bian G-L, Wei L-C, Chen L-W, Cao R (2007) Fluoro-Jade C can specifically stain the degenerative neurons in the substantia nigra of the 1-methy-4-phenyl-1,2,3,6-tetrahydro pyrindine-treated C57BL/6 mice. Brain Res 1150:55–61 DOI: 10.1016/j.brainres.2007.02.078.

Shi R, Weng J, Zhao L, Li XM, Gao TM, Kong J (2012) Excessive Autophagy Contributes to Neuron Death in Cerebral Ischemia. CNS Neurosci Ther

18:250–260 DOI: 10.1111/j.1755-5949.2012.00295.x.

Susan E (2007) Apoptosis: A Reveiw of Programmed Cell Death. Toxicol Pathol 35:496–516 DOI: 10.1080/01926230701320337.

Takamori Y, Wakabayashi T, Mori T, Kosaka J, Yamada H (2014) Organization and Cellular Arrangement of Two Neurogenic Regions in the Adult Ferret (Mustela putorius furo) Brain. 1838:1818–1838 DOI: 10.1002/cne.23503.

Tamamaki N, Nakamura K, Okamoto K, Kaneko T (2001) Radial glia is a progenitor of neocortical neurons in the developing cerebral cortex. Neurosci Res 41:51–60 DOI: 10.1016/s0168-0102(01)00259-0.

Tamamaki N, Yanagawa Y, Tomioka R, Miyazaki JI, Obata K, Kaneko T (2003) Green Fluorescent Protein Expression and Colocalization with Calretinin, Parvalbumin, and Somatostatin in the GAD67-GFP Knock-In Mouse. J Comp Neurol 467:60–79 DOI: 10.1002/cne.10905.

Vermillion KL, Lidberg KA, Gammill LS (2014) Expression of actin-binding proteins and requirement for actin-depolymerizing factor in chick neural crest cells. Dev Dyn 243:730–738 DOI: 10.1038/jid.2014.371.

Wang L, Liu YH, Huang YG, Chen LW (2008) Time-course of neuronal death in the mouse pilocarpine model of chronic epilepsy using Fluoro-Jade C staining. Brain Res 1241:157–167 DOI: 10.1016/j.brainres.2008.07.097.

William S, III NM, Tao C (2004) N-Ethyl-N-nitrosourea (ENU) Increased Brain Mutations in Prenatal and Neonatal Mice but Not in the Adults. Toxicol Sci 81:112–120 DOI: 10.1093/toxsci/kfh177.

Yamanaka H, Kobayashi K, Okubo M, Fukuoka T, Noguchi K (2011) Increase of close homolog of cell adhesion molecule L1 in primary afferent by nerve injury and the contribution to neuropathic pain. J

Comp Neurol 519:1597–1615 DOI: 10.1002/cne.22588.